A Simple Approach to Attosecond Electronic Chirality Flips Using Triatomic Molecules – Supplementary Information

Dietrich Haase,[†] Jörn Manz,[*,†] Beate Paulus,[†] Jonathan Scherlitzki,[†] and Jean Christophe Tremblay[*,‡]

[†]*Institut für Chemie und Biochemie, Freie Universität Berlin, 14195 Berlin, Germany*

[‡]*LPCT, Université de Lorraine, 57000 Metz, France*

E-mail: jmanz@chemie.fu-berlin.de; jean-christophe.tremblay@univ-lorraine.fr

Contents

S1 Electronic Properties of NSF

All quantum chemical calculations on thiazyl fluoride (NSF) were performed at the Complete Active Space Self-Consistent Field (CASSCF) level of theory, as implemented in the software package Molpro, version 2021.3.[1] A CAS(18,12) with an aug-cc-pVTZ basis[2] on all atoms was used. For higher accuracy, we set the convergence threshold for energy to 1×10^{-9} a. u., for orbitals to 1×10^{-7} a. u., and for orbital gradients to 1×10^{-6} a. u. The presented results were obtained by averaging the lowest state of A'- and the lowest two states of A''-symmetry, all of them with equal weights. We will use (1,2)-SA-CASSCF[3] to denote this method. In addition, SS-CASSCF[4,5] refers to state-specific CASSCF(18,12) computations which were used as a reference whenever (1,2)-SA-CASSCF results were not available.

First, the NSF structure known in the literature[6] is optimized in the ground and first electronic excited states, applying accurate convergence criteria of 1×10^{-9} a. u. for energy, 1×10^{-6} a. u. for optimization gradients, and 1×10^{-4} a. u. for structure optimization steps. A normal mode analysis was then performed in the C_1 point group. Tables S1, S2, and S3 provide an overview on the relevant results.

Table S1: Minimum geometries and energies

state	Φ [°]	r(F − S) [Å]	r(S − N) [Å]	ΔE_{min} [eV]	ZPE [eV]
			(1,2)-SA-CASSCF		
$1A'$	115.8	1.652	1.467	0	0.147
$1A''$	102.1	1.652	1.603	3.294	—
			SS-CASSCF		
$1A'$	115.7	1.651	1.460	0	0.149
$1A''$	102.2	1.633	1.604	3.415	0.118

Table S2: Normal mode frequencies and intensities

state	$\tilde{\nu}_1$ [cm^{-1}]	$\tilde{\nu}_2$ [cm^{-1}]	$\tilde{\nu}_3$ [cm^{-1}]	I_1 [kJ mol^{-1}]	I_2 [kJ mol^{-1}]	I_3 [kJ mol^{-1}]
			(1,2)-SA-CASSCF			
$1A'$	380.07	653.03	1337.46	14.03	168.42	4.69
			SS-CASSCF			
$1A'$	387.86	647.98	1361.22	16.25	235.58	20.91
$1A''$	319.59	676.92	907.09	10.13	161.05	2.82

Table S3: Vertical excitation energies and transition dipole moments at (1,2)-SA-CASSCF level

m	$\Delta E = E(mA'') - E(1A')$ [eV]	$\langle 1A' \vert \mu_z \vert mA'' \rangle$[Db]
1	3.745	−0.416
2	5.843	0.062

S2 Derivation of the Dominant Determinants Approximation

The contribution of different electronic configurations to the total N-electron wavefunction is given in table S4. Each of them can be interpreted as a normalized Hartree product $\Phi_I(\mathbf{r}^N) = \sqrt{N!}\prod_{n=1}^{N}\chi_m^{\varsigma}(\mathbf{r}_n)$ of all occupied spin orbitals χ_m^{ς}, $m = 1, 2, \ldots$ and $\varsigma \in \{\alpha, \beta\}$, acted on by the unitary antisymmetrization operator $\mathcal{A} = (N!)^{-1}\sum_{P\in S_N}\mathrm{sgn}(P)\,P$ for the set of permutations S_N. The (1,2)-SA-CASSCF results show that the ground state is dominated by the lowest-lying closed-shell Slater determinant of the form

$$\Phi_{\ldots 22}(\mathbf{r}^N) = \sqrt{N!}\ldots\chi^{\alpha}_{\mathrm{HOMO}-1}(\mathbf{r}_{N-3})\chi^{\beta}_{\mathrm{HOMO}-1}(\mathbf{r}_{N-2})\chi^{\alpha}_{\mathrm{HOMO}}(\mathbf{r}_{N-1})\chi^{\beta}_{\mathrm{HOMO}}(\mathbf{r}_N) \tag{1}$$

where, in the present case, HOMO refers to the 16-th orbital. The normalisation of the wave function was chosen such that the density integrates to the number of electrons, i.e. $\int \Phi_{\ldots 22}(\mathbf{r}^N)\Phi_{\ldots 22}(\mathbf{r}^N)d\mathbf{r}^N = N$. Analogously, by denoting the 17-th orbital as LUMO, the two main Slater determinant contributions

$$\Phi_{\ldots 2\alpha\beta}(\mathbf{r}^N) = \sqrt{N!}\ldots\chi^{\alpha}_{\mathrm{HOMO}-1}(\mathbf{r}_{N-3})\chi^{\beta}_{\mathrm{HOMO}-1}(\mathbf{r}_{N-2})\chi^{\alpha}_{\mathrm{HOMO}}(\mathbf{r}_{N-1})\chi^{\beta}_{\mathrm{LUMO}}(\mathbf{r}_N), \text{ and} \tag{2}$$

$$\Phi_{\ldots 2\beta\alpha}(\mathbf{r}^N) = \sqrt{N!}\ldots\chi^{\alpha}_{\mathrm{HOMO}-1}(\mathbf{r}_{N-3})\chi^{\beta}_{\mathrm{HOMO}-1}(\mathbf{r}_{N-2})\chi^{\beta}_{\mathrm{HOMO}}(\mathbf{r}_{N-1})\chi^{\alpha}_{\mathrm{LUMO}}(\mathbf{r}_N) \tag{3}$$

equally determine the first excited state. Thus, it is valid to approximate equation (7) of the main text as

$$|\psi(t)\rangle = \sqrt{N!}c_{A'}e^{i\delta_{A'}}\mathcal{A}\,|\Phi_{\ldots 22}\rangle + \sqrt{N!}c_{A''}e^{i\delta_{A''}}\left[\sqrt{\frac{1}{2}}\mathcal{A}\,|\Phi_{\ldots 2\alpha\beta}\rangle + \sqrt{\frac{1}{2}}\mathcal{A}\,|\Phi_{\ldots 2\beta\alpha}\rangle\right]e^{-i\omega t}. \tag{4}$$

Accordingly, the cross-term contribution to the density, defined in equation (11), gives

$$\varrho_{A'A''}(\mathbf{r}) = \sqrt{\frac{1}{2}}\left(\langle\Phi_{\ldots 22}|\sum_{k=1}^{N}\delta(\mathbf{r}_k-\mathbf{r})|\Phi_{\ldots 2\alpha\beta}\rangle + \langle\Phi_{\ldots 22}|\sum_{k=1}^{N}\delta(\mathbf{r}_k-\mathbf{r})|\Phi_{\ldots 2\beta\alpha}\rangle\right). \tag{5}$$

Both terms on the r.h.s. are transition moments of a one-electron operator between Slater determinants that differ by one spin orbital. Consequently, the expression can be simplified using the Slater-Condon rules in terms of one-electron integrals.[7–9] This leads to the following simplified form upon integration over all spin

$$\varrho_{A'A''}(\mathbf{r}) = \sqrt{2}\int_{\mathbb{R}}\phi_{\mathrm{HOMO}}(\mathbf{r}')\delta(\mathbf{r}'-\mathbf{r})\phi_{\mathrm{LUMO}}(\mathbf{r}')\,\mathrm{d}\mathbf{r}' \tag{6}$$

where we introduced the spatial molecular orbitals $\phi_m(\mathbf{r})$. Finally,

$$\varrho_{A'A''}(\mathbf{r}) = \sqrt{2}\phi_{\mathrm{HOMO}}(\mathbf{r})\phi_{\mathrm{LUMO}}(\mathbf{r}) \tag{7}$$

Table S4: CI coefficients for the lowest states of NSF in ground state minimum geometry on (1,2)-SA-CASSCF level. Orbitals 12, 14, and 17 are A''-symmetric, the remaining orbitals A'-symmetric

	occupation scheme												coefficient
	8	9	10	11	12	13	14	15	16	17	18	19	
$1A'$	2	2	2	2	2	2	2	2	2	0	0	0	0.949 608 40
	2	2	2	2	2	2	0	2	2	2	0	0	−0.150 501 99
	2	2	2	2	2	2	2	2	0	0	2	0	−0.086 639 15
	2	2	2	2	2	2	α	2	β	β	α	0	0.068 031 78
	2	2	2	2	2	2	β	2	α	α	β	0	0.068 031 78
	2	2	2	2	2	0	2	2	2	0	2	0	−0.054 939 79
$1A''$	2	2	2	2	2	2	2	2	α	β	0	0	−0.661 100 47
	2	2	2	2	2	2	2	2	β	α	0	0	0.661 100 47
	2	2	2	2	2	2	2	α	2	β	0	0	−0.168 527 89
	2	2	2	2	2	2	2	β	2	α	0	0	0.168 527 89
	2	2	2	2	2	α	β	2	2	2	0	0	−0.048 700 80
	2	2	2	2	2	β	α	2	2	2	0	0	0.048 700 80
	2	2	2	2	2	2	2	α	0	β	2	0	0.018 504 36
	2	2	2	2	2	2	2	β	0	α	2	0	−0.018 504 36
	2	2	2	α	2	2	β	2	2	2	0	0	−0.010 369 49
	2	2	2	β	2	2	α	2	2	2	0	0	0.010 369 49

S3 Time Evolution of the Nuclear Wavefunction

Using (1,2)-SA-CASSCF, the ground state and excited state potential energy hypersurfaces (PES) were determined on the points of a regular grid of Jacobi coordinates, as illustrated in figure S1. The parameters defining this grid are given in table S5. Both, the $1A'$- and the

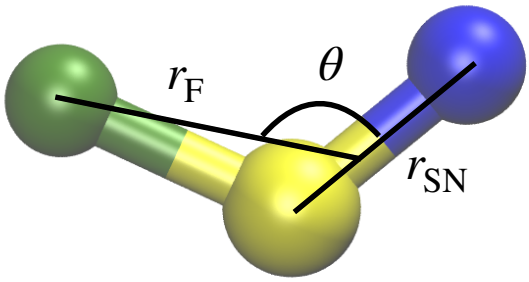

Figure S1: Definition of the Jacobi coordinates used for the nuclear dynamics simulations. Fluorine in green, sulfur in yellow, nitrogen in blue.

A''-surface, were then fitted using the PotFit program,[10] version 8.6, by contracting over the angular degree of freedom θ.

Table S5: Grid parameters

	θ	r_F	r_{SN}
lower boundary	85°	1.4 Å	1.2 Å
upper boundary	150°	2.7 Å	2.2 Å
number of points	14	14	11

Table S6: DVR parameters

	θ	r_F	r_{SN}
DVR type	restricted Legendre	Colbert-Miller	Hermite
first point x_1	85°	1.4 Å	1.2 Å
last point x_N	150°	2.7 Å	2.2 Å
number of points	216/80	80	80

To obtain a refined discrete variable presentation (DVR), the PotFit output was further processed with chnpot, version 8.6.[10] This program performed a cubic-spline interpolation to map the PES on the DVR given in table S6.

An initial wavepacket was then optimized on the ground state PES by propagating a starting guess, a Hartree product of three Gauss functions centered in the ground state minimum with widths corresponding to the $1A'$ normal mode frequencies, in imaginary time. To this end, the keyword RELAXATION of the Heidelberg MCTDH program package was utilized.[10]

Finally, we performed a 40 fs-real-time propagation of this initial wavepacket on the $1A''$ surface, with output every 0.5 fs. Snapshots of this propagation are shown in figures S2, S3, and S4.

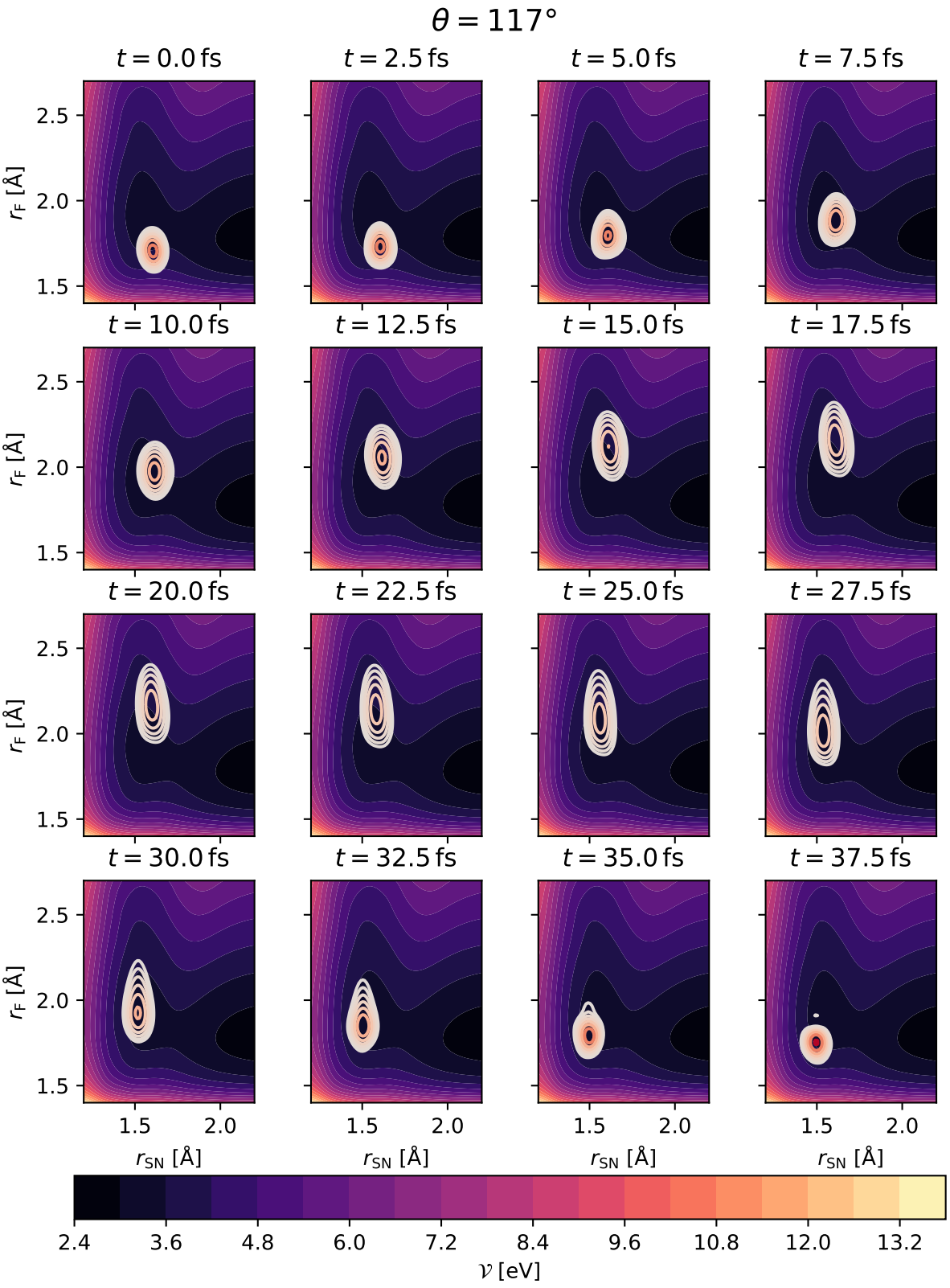

Figure S2: Wave packet (isocontours) on the $1A''$-PES cross-section (color map) at $\theta = 117°$. 8 isolines logarithmically sampled between 1 a. u. and 1.451 a. u.

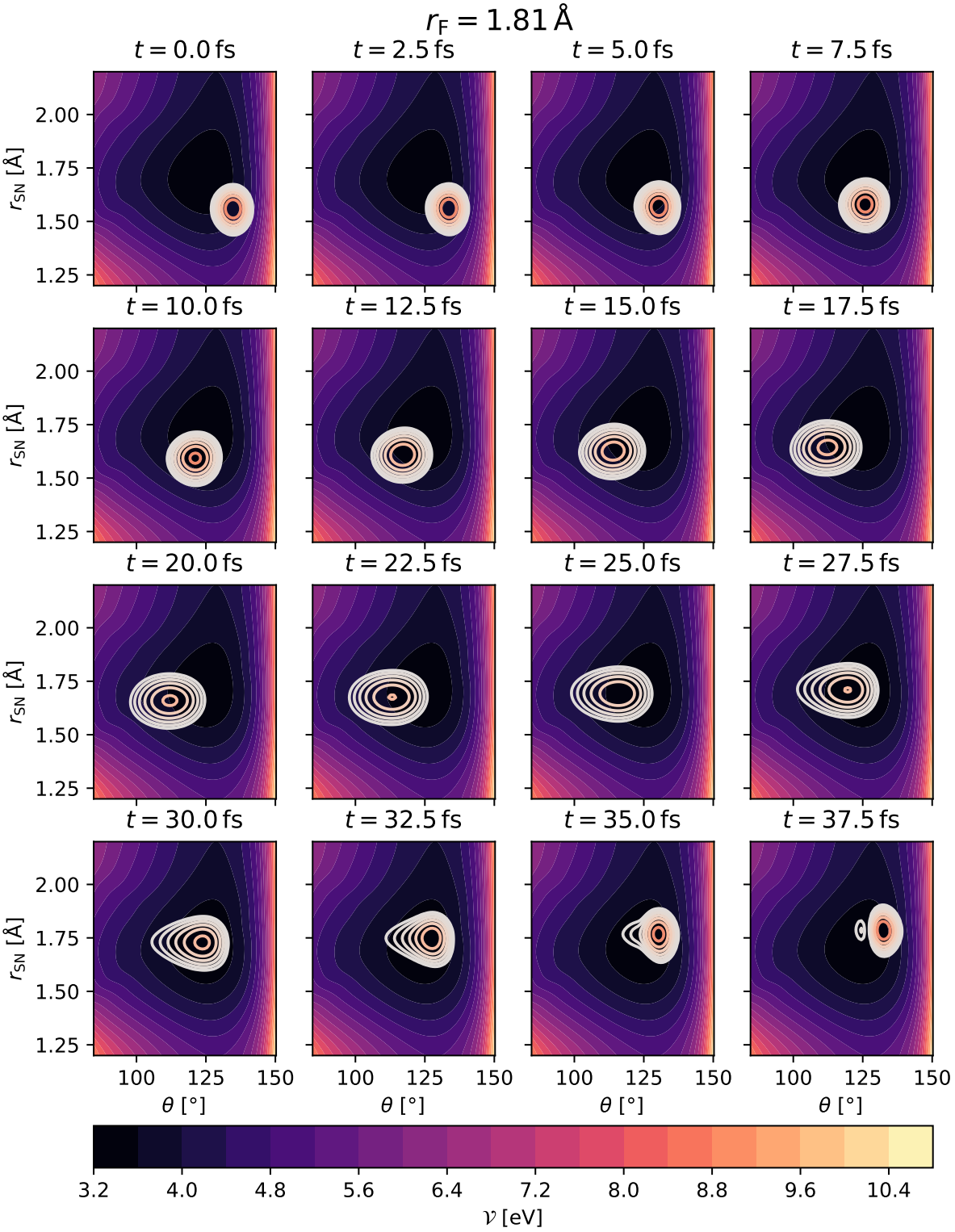

Figure S3: Wave packet on the $1A''$-PES cross-section at $r_F = 1.81$ Å. 8 isolines logarithmically sampled between 1 a. u. and 1.735 a. u.

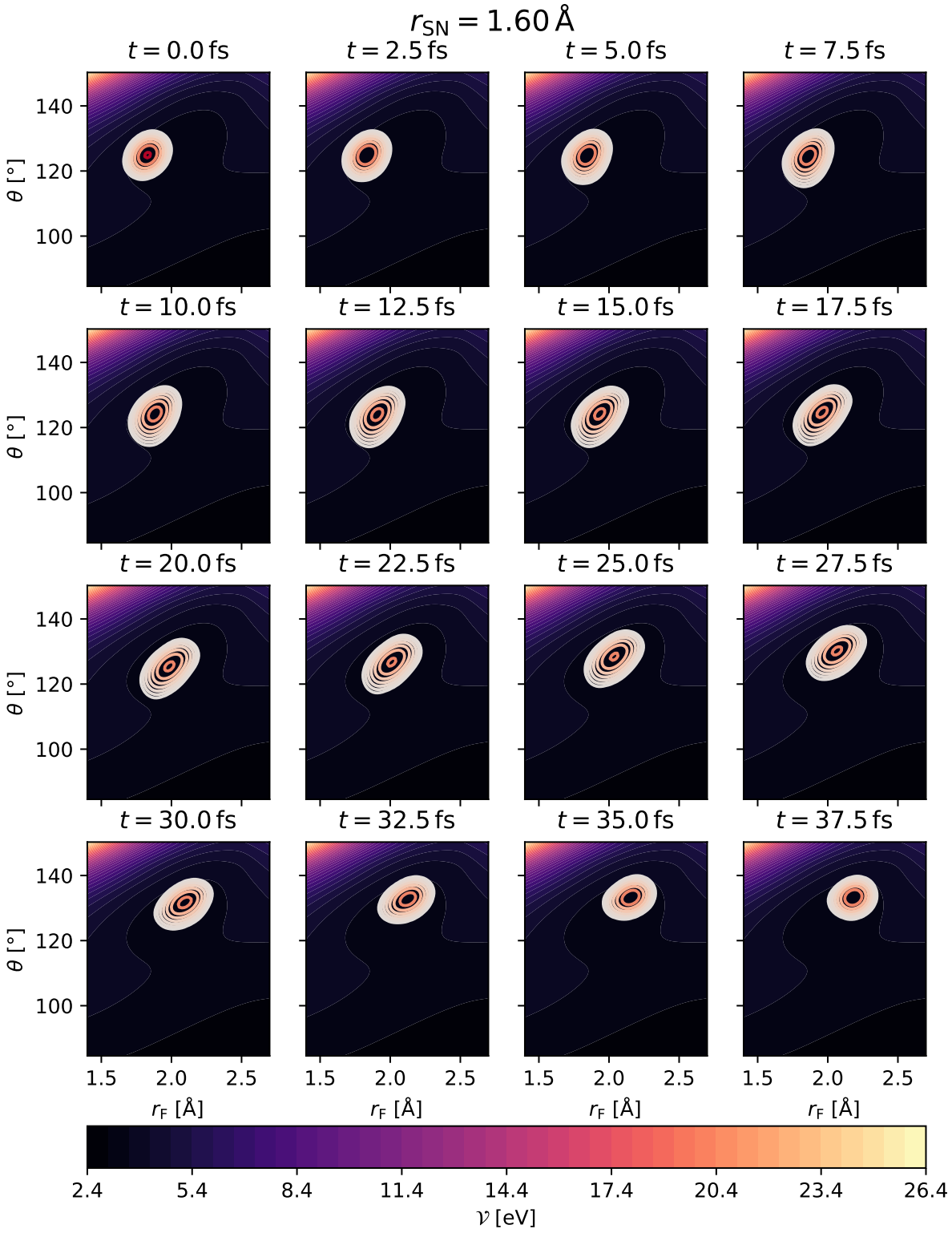

Figure S4: Wave packet on the $1A''$-PES cross-section at $r_{SN} = 1.60$ Å. 8 isolines logarithmically sampled between 1 a. u. and 1.532 a. u.

References

(1) Werner, H.-J.; Knowles, P. J.; Manby, F. R.; Black, J. A.; Doll, K.; Heßelmann, A.; Kats, D.; Köhn, A.; Korona, T.; Kreplin, D.; et. al. The Molpro quantum chemistry package. 2020.

(2) Dunning Jr, T. H.; Peterson, K. A.; Wilson, A. K. Gaussian basis sets for use in correlated molecular calculations. X. The atoms aluminum through argon revisited. *J. Chem. Phys.* **2001**, *114*, 9244–9253.

(3) Werner, H.-J.; Meyer, W. A quadratically convergent MCSCF method for the simultaneous optimization of several states. *J. Chem. Phys.* **1981**, *74*, 5794–5801.

(4) Dalgaard, E. Time-dependent multiconfigurational Hartree–Fock theory. *J. Chem. Phys.* **1980**, *72*, 816–823.

(5) Olsen, J.; Jørgensen, P. Linear and nonlinear response functions for an exact state and for an MCSCF state. *J. Chem. Phys.* **1985**, *82*, 3235–3264.

(6) Schaad, L. J.; Hess, B. A.; Carsky, P.; Zahradnik, R. Ab initio studies on the ground state potential surface and vibrational spectra of NSF and SNF. **1984**, *23*, 2428–2430.

(7) Slater, J. C. The theory of complex spectra. *Phys. Rev.* **1929**, *34*, 1293.

(8) Condon, E. The theory of complex spectra. *Phys. Rev.* **1930**, *36*, 1121.

(9) Slater, J. C. Molecular energy levels and valence bonds. *Phys. Rev.* **1931**, *38*, 1109.

(10) Beck, M. H.; Jäckle, A.; Worth, G. A.; Meyer, H.-D. The multiconfiguration time-dependent Hartree (MCTDH) method: a highly efficient algorithm for propagating wavepackets. *Phys. Rep.* **2000**, *324*, 1–105.